JOURNAL OF MATERIALS SCIENCE 25 (1990) 4001–4007

The deformation of brittle starch foams

S. C. WARBURTON, A. M. DONALD
Cavendish Laboratory, Madingley Road, Cambridge, CB3 OHE, UK
A. C. SMITH
Institute of Food Research, Colney Lane, Norwich, NR4 7UA, UK

There exists a theoretical model to describe the deformation of solid foams which relates the mechanical properties to the foam density and the cell-wall properties. Previous work has assumed that the wall properties are constant for a wide range of different density foams and can be characterized by the properties of the unfoamed material. In this paper we show that, when considering extruded starch foams, variation of the extrusion parameters in order to produce different bulk density foams has an effect on the cell-wall material: notably upon the crystallinity, T_g and wall density. Therefore, both the bulk foam and cell-wall mechanical properties were measured in order to test the full theory. For the relative fracture stress, excellent agreement was found between the predicted power law behaviour and the experimental results. However, the power law for the relative modulus is larger than the predicted value.

1. Introduction

The deformation of solid foams has become a subject of great interest following the publications of Gibson, Ashby and colleagues [1–4] which describe the modelling of foams and their response to applied forces. They have shown that the dominant physical characteristic of a solid foam is its relative density: that is, the density of the foam divided by the density of the solid from which it is made. The theory predicts scaling laws between the physical properties of a foam, such as Young's modulus and fracture stress, and the relative density. For example

$$\frac{E^*}{E_s} \propto \left(\frac{\rho^*}{\rho_s}\right)^m \quad (1)$$

$$\frac{\sigma_f^*}{\sigma_f} \propto \left(\frac{\rho^*}{\rho_s}\right)^n \quad (2)$$

where E^* is the Young's modulus of the foam, E_s is the Young's modulus of the cell-wall material, σ_f^* is the fracture stress of the foam, σ_f is the fracture stress of the cell-wall material, ρ^* is the foam density, and $\rho_s$the density of the cell walls. The power laws depend upon whether the foams are open-celled or close-celled (whether the cells are interconnected or not). For open cells, $m = 2$ and $n = 3/2$, and for closed cells, $m = 3$ and $n = 2$.

Experimental verification of these predictions [2] has used the assumption that the foams' cell walls can be characterized by the physical properties of the unfoamed material. This presumes that the properties are unaltered during the foaming process and remain constant across a range of different density foams made from the same material. For synthetic polymers these assumptions seem justified as there is good agreement between experiment and theory. The physical properties of polyethylene, for example, are well characterized and do not vary significantly under different foaming conditions.

However, constancy of properties under different foaming conditions need not be the case. In the present work we aimed to test the full theory by measuring the cell wall properties of each specimen, as well as the bulk foam properties. The system under study is based upon extruded maize starch in the form of maize grits. When extruded, starch undergoes transformations described below, which vary according to the extrusion conditions. For this reason it seems unlikely that different density foams will possess cell walls of identical character. An additional point of interest for the starch foams is that they are brittle, and to date very little literature exists on brittle foams for comparison with theory.

Starch is a polysaccharide containing repeated glucose units $(C_6H_{10}O_5)_x$. It consists of two primary components: amylose is a mainly linear molecule, with a molecular weight of $\approx 10^4$ and amylopectin is a branched molecule, with a molecular weight of $\approx 10^8$. Native starch exists as granules which also contain varying proportions of lipids, proteins and ash, depending upon the source of the starch [5]. The granules resemble spherulites, with both crystalline and amorphous areas [6]. They exhibit birefringence and produce characteristic X-ray spectra. When heated in the presence of water the granules undergo gelatinization. Initially the granules swell and the starch becomes hydrated, then a viscous paste is formed as the amylose molecules are leached from the granules to form a continuous matrix [5]. Gelatinization results in a loss of birefringence and a reduction in crystallinity [7]. The temperature at which this occurs is approximately 60° C but depends upon the

0022–2461/90 $03.00 + .12

TABLE I Summary of the extrusion conditions under which the solid foams were made

Sample	Barrel temperature profile (° C)	Die temperature (° C)	Water content (% weight for weight basis (w.w.b.))
1	25–52–80–100–120	126	22.3
2	25–52–80–100–120	127	20.2
3	25–52–80–100–120	129	18.3
4	25–52–80–100–120	133	16.1
5	25–52–80–100–120	139	13.7
6	25–52–80–100–120	144	12.6
7	25–57–100–120–140	139	16.1
8	25–70–120–140–160	150	16.1
9	32–93–160–180–200	170	16.1

variety of starch and also upon the amount of water present [5]. Starch also exhibits a glass transition, the temperature of which (T_g) again varies with water content. T_g increases with a decreasing amount of water present and ranges from below room temperature, at more than 22% moisture content, to above 100° C, at 10% moisture content and less [8].

When starch is extruded with water to produce a foamed structure, the granules are subject to high temperatures and shearing forces within the extruder barrel. The granule structure is disrupted as gelatinization occurs and a viscous dough is produced [9]. The pressure in the barrel causes the water to become superheated and, as the dough emerges from the die, the resulting pressure drop turns the water to steam and foaming takes place. The foams solidify as they cool and pass through T_g. In order to produce a set of foams of different relative densities the extrusion conditions must be varied, for example by changing the barrel temperature or water content. These variables will, however, affect the extent of granule breakdown, and hence also affect the properties of the cell walls. For instance, the glass transition temperature of the starch in our experimental foams was not constant across the set because the lower density foams were created by reducing the water content of extrusion. Furthermore, the crystallinity of the cell wall material changes with extrusion conditions [10]. Not only will this alter the ratio of the amorphous to the crystalline material, but different amylose–lipid complexes may be formed. For cereal starch two complexes exist, known as the V_h and E_h forms, consisting of lipids within an amylose double helix but with different interaxial spacings. The former is the stable complex and the latter has been found in extrudates made at high temperatures [11]. The degree of molecular degradation is also dependent upon the extrusion conditions; for example, the higher the extrusion temperature the more degradation takes place [12]. For all these reasons it seems unreasonable to assume that the cell wall properties of starch foams are constant across a range of different density foams.

2. Experimental procedure

2.1. Specimens

The solid foams were made from extruded maize grits and water, using a Baker Perkins MPF 50D co-rotating twin screw extruder. Two sets of foams were created; one extruded at constant barrel temperature and varying water content, the other at constant water content and varying barrel temperature. The extrusion conditions are summarized in Table I. Two circular 6 mm diameter dies were used, which produced cylindrical samples with diameters ranging from approximately 15 to 25 mm. The screw speed and feed rate were kept constant at 250 r.p.m. and 30 kg h^{-1} respectively. The foams were dried and stored in an oven at 40° C.

2.2. Characterization

The extruded foams were all closed-cell foams; that is, the cells were not interconnected. Fig. 1 shows photographs of each sample, cut perpendicular to the extrusion direction and gold plated for use in the SEM. There was no obvious anisotropy contained within the foams. The cell-size distributions and average cell sizes were calculated from the measurements of the maximum diameters of 100 cells via image analysis of photographs taken with a 1 : 1 macro-lens. The cell-wall thicknesses were measured from scanning electron micrographs of 50 cell walls per sample. The results are given in Table II.

2.3. Differential scanning calorimetry (DSC)

Foam samples were ground, both immediately after extrusion and after drying at 40° C, and placed in preweighed aluminium DSC crucibles. These were hermetically sealed and reweighed in order to determine the sample mass. Approximately 20 mg of each sample was used and four samples per specimen were tested. The specimens were heated in a Mettler TA3000 differential scanning calorimeter from 25 to 260° C at a rate of 10° C min^{-1} and with a full scale depletion (f.s.d.) of 10 mW. An empty aluminium crucible was used for the reference. Data was analysed with the TA 10 30 software in order to determine the T_g. The values quoted in Table II are the mid-points of the glass transition.

TABLE II Summary of the foam characterization and DSC results

Sample	Average cell size (mm)	Average cell-wall thickness (mm)	T_g (° C)
1	2.3 (1.3)	165 (120)	67
2	2.2 (1.2)	120 (65)	80
3	2.4 (1.4)	125 (90)	96
4	2.6 (1.6)	90 (60)	101
5	2.3 (1.7)	45 (20)	–
6	2.0 (1.1)	60 (40)	–
7	2.6 (1.7)	70 (45)	104
8	2.9 (1.8)	55 (35)	104
9	2.6 (1.7)	70 (45)	112

Figures in brackets indicate standard deviations.

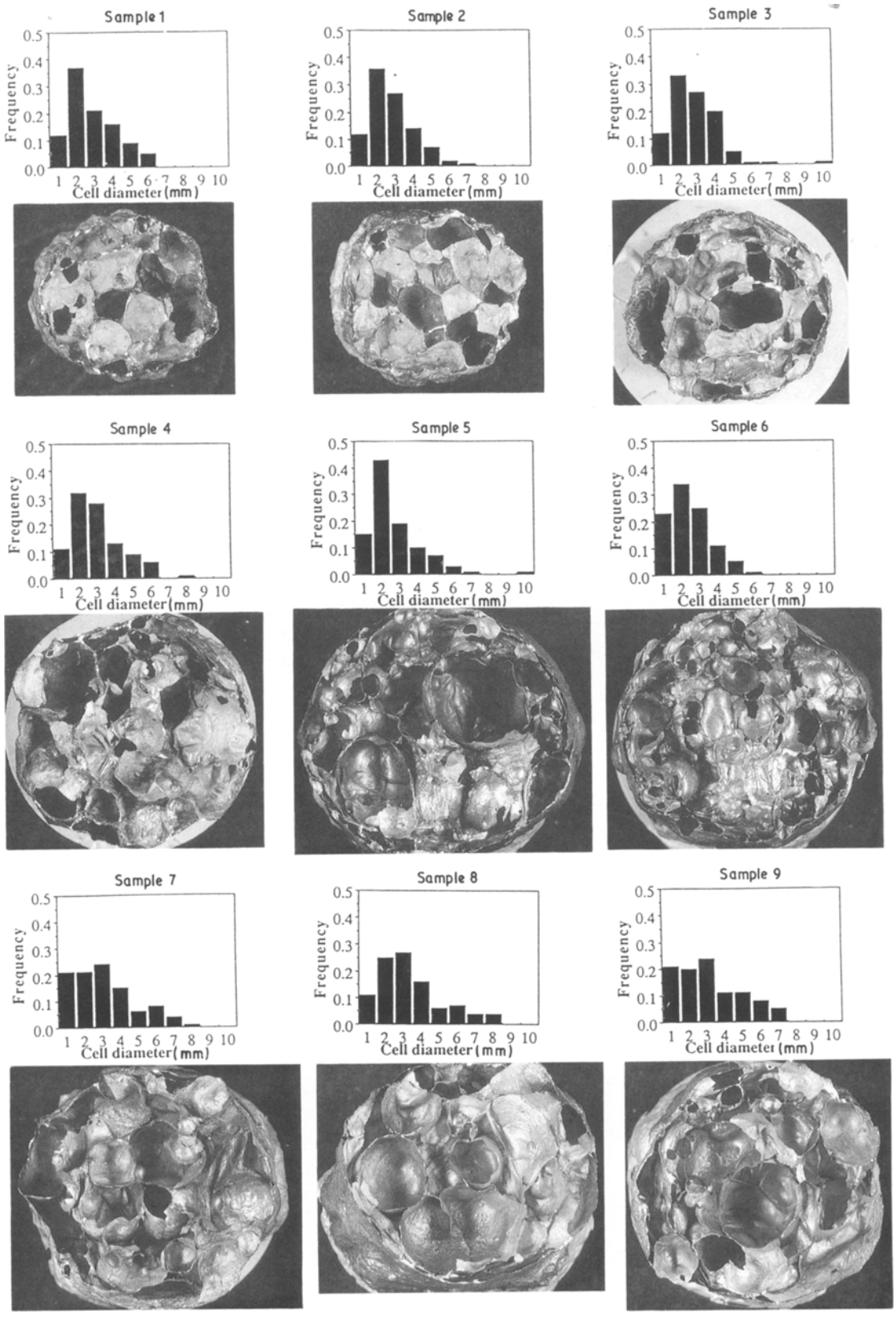

Figure 1 Photographs of the maize foams (cut perpendicular to the extrusion direction and gold-plated) and the cell-size distributions for each sample.

2.4. X-ray diffraction

The samples were ground after drying and mounted in 0.3 mm glass capillaries. X-ray diffraction patterns of each specimen were produced with a Debye–Scherrer camera using Cu$K\alpha$ radiation. The positions of the diffraction peaks were measured to determine the presence of amylose–lipid complexes.

2.5. Relative densities

The bulk densities were calculated assuming that a length of foam was cylindrical. The sample was weighed, its length and diameter determined from ten measurements of each using calipers, and the density was then determined. The validity of this assumption was based upon the fact that the results agreed within

experimental error to those calculated via sand displacement measurements. This latter method determined the volume of the foams by the displacement of a known volume of fine sand, but was not as simple to perform, owing to the fact that some sand entered through holes in the foam walls, and the uncertainty in whether the sand particles had fully settled.

The cell wall densities were determined via the displacement of toluene in $2\,cm^3$ measuring flasks. Approximately 0.5 g of wall material was used per measurement and the average of five results per foam sample was calculated. Pieces of cell wall were cut from the foam and placed in a preweighed flask of mass m_1. The flask was reweighed, to give mass m_2, and then filled to the calibrated level with toluene and weighed again, this being mass m_3. The three masses and the density of toluene were used to calculate the density of the wall material from the following equation

$$\rho_s = \frac{(m_2 - m_1)\rho_{tol}}{V\rho_{tol} - m_3 + m_2} \quad (3)$$

where ρ_s is the cell wall density, ρ_{tol} the density of toluene at room temperature and V is the volume of the measuring flask.

2.6. Mechanical properties

To determine the Young's moduli and fracture stresses of the bulk foams, the samples were cut into approximately 2 cm lengths using a rotary saw. The actual lengths and diameters of these cylindrical samples were calculated from ten measurements of each with calipers. The foams were then deformed in uniaxial compression with an Instron 1122, using a 500 kg load cell and a cross-head speed of $5\,mm\,min^{-1}$. The foams were compressed between two pieces of 6 mm thick elastomeric foam so as to distribute the forces evenly over the rough surface of the sample. This prevented a large stress being applied to a small protrusion. The fracture stress was found simply from the load to failure divided by the circular cross-sectional area of the foam. The modulus was determined from the gradient of the linear part of the force–displacement curve before failure, but had to be corrected in order to remove the contribution from the elastomeric foam. Considering the foams in series, and using the facts that the displacements are additive and the stress is uniform, produces the equation

$$\frac{2l_e + l^*}{E} = \frac{2l_e}{E_e} + \frac{l^*}{E^*} \quad (4)$$

where l^* is the sample foam length, E^* is the sample foam modulus, l_e is the elastomeric foam thickness, E_e is the elastomeric foam modulus, and E is the combined modulus, determined from the gradient. E_e was found by compressing a steel cylinder of known modulus, and of similar dimensions to the sample foam, between the elastomeric foam. The gradient for this force–displacement curve was measured at the same stress as that for the sample foam. Using a similar equation to that above, but this time involving the steel cylinder length and modulus rather than those of the sample foam, and the appropriate combined modulus, yields E_e and hence E^*.

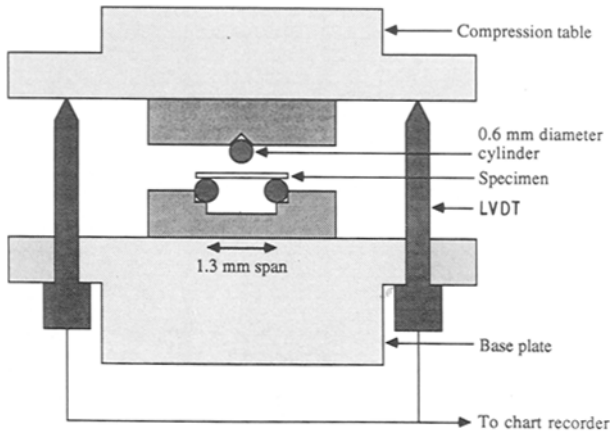

Figure 2 A diagram of the three-point bend apparatus used to measure the mechanical properties of the foam cell walls.

The cell-wall properties were determined by performing a three-point bend test upon a flat rectangular piece of wall, approximately 3 mm × 1 mm × 0.1 mm in size. These were cut with a scalpel from the foam. The actual width was found by using a travelling microscope and the thickness was measured, after testing, with a micrometer. The specimens were loaded into the rig with a 1.3 mm span, as shown schematically in Fig. 2. A load cell of 1 kg and cross-head speed of $0.5\,mm\,min^{-1}$ were used. The displacement measured via the linear voltage displacement transducers (LVDTs) was calibrated with glass cover slips of known thickness and distances as small as 1 μm could be measured. The wall modulus, E_s, and wall fracture stress, σ_f, were calculated from the standard equations [13] given below

$$E_s = \frac{L^3 F}{4bh^3 Y} \quad (5)$$

$$\sigma_f = \frac{3F_f L}{2bh^2} \quad (6)$$

where L is the span between the three-point bend supports, b is the specimen width, h is the specimen thickness, Y is the displacement, F is the load applied and F_f is the load to failure.

Samples of sheet polytetrafluoroethylene (PTFE), with similar dimensions to the cell wall specimens, were used to calibrate the values of the wall moduli calculated from the three-point bend test apparatus. Owing to the unknown stress concentrations around the supports it was found that the measured modulus of the PTFE was consistently ten times lower than the true value. For this reason we applied a correction factor of × 10 to all cell wall moduli. This does not alter the gradient of the graph of log relative modulus against log relative density.

3. Results and discussion

The results of the mechanical tests are summarized in Table III. Sample 5 has no recorded cell wall properties because the walls yielded plastically rather than fractured in the three-point bend tests. This was most probably due to the very thin cell walls (45 μm) which required a narrower span: the British Standard's

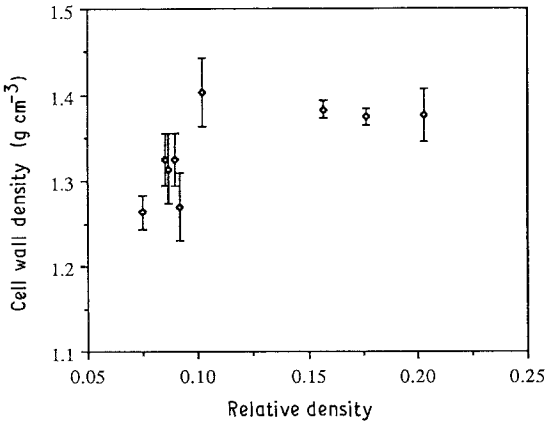

Figure 3 The variation of cell-wall density with relative density.

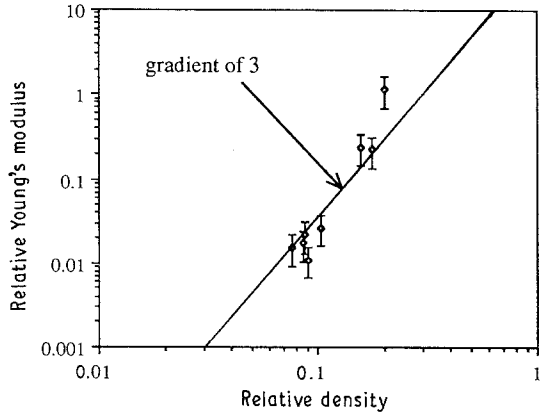

Figure 4 The log relative modulus as a function of log relative density. The theoretical prediction is denoted by the solid line.

recommendation is for the span to be 15 to 17 times the specimen thickness [13].

The DSC results in Table II show the variation of T_g with extrusion conditions. The results are taken from the samples before drying because at the very low water contents of the dried samples the magnitude of the glass transition became imperceptibly small. As the water content added to the maize during extrusion is reduced from 22.3% (sample 1) to 16.1% (sample 6) the T_g rises from 67° C to over 101° C. It was not possible to measure the T_g for samples 5 and 6 because the transition became coincident with the melting peak of the amylose–lipid complex crystallites and was thus obscured. As expected, results also indicated a rise in T_g with an increase in barrel temperature. This is because a higher barrel temperature leads to foams of lower moisture content, because more superheating occurs and so more water flashes off when foaming takes place. Water acts as a plasticizing agent [14] and, as with conventional polymers, a decrease in the plasticizer concentration raises the T_g. The crystallinity of the polymer can also affect T_g [15].

All samples showed the presence of both V_h and E_h complexes. However, at the high water contents (samples 1 to 3), the V_h diffraction peaks dominated and the E_h peaks were very weak. As the water content was reduced, the intensity of the E_h peaks increased and the V_h intensity decreased, and by sample 5 the E_h diffraction peaks were stronger than the V_h. The same trend occurred as the die temperature was raised: sample 7 (die temperature of 140° C) contained more intense V_h peaks, whereas in sample 9 (die temperature of 200° C) the E_h peaks were stronger.

It can be seen that there is a significant variation in the cell-wall density over the range of foams tested. Fig. 3 shows how the density of the cell walls falls with a reduction in the relative density of the foams. It seems likely that this can be attributed, at least in part, to the fact that as more expansion takes place during the foaming process, isolated bubbles are produced within the cell walls themselves. This is supported by the fact that when the samples were ground to a fine powder while measuring the cell wall densities (as opposed to using pieces of the walls) all sample densities approached 1.47 g cm^{-3}, the value for the density for starch [16]. Air spaces of 5 μm and less have been recorded from TEM work on starch extrudate wall [17].

Within experimental error it was not possible to detect a variation in the cell-wall moduli or fracture stresses. However, because the mechanical properties of extruded starch are not well characterized, the experiments served a useful purpose in determining these values. Any possible differences in the wall properties that may have existed were masked by the size of the errors: no values differed by more than two standard deviations. In performing these experiments one possible source of errors could be that cracks were introduced into the wall specimens when cut. This would lead to a reduction in the wall moduli and fracture stresses. Another point to note is that measurements of the wall thickness with a micrometer will overestimate the true value. Because the wall modulus is inversely proportional to the cube of the wall thickness, and the fracture stress inversely

TABLE III Experimental results from the mechanical testing of the bulk foams and the cell walls

Sample	Foam density (g cm^{-3})	Cell-wall density (g cm^{-3})	Foam Young's modulus (MPa)	Cell-wall modulus (GPa)	Foam fracture stress (MPa)	Cell-wall fracture stress (MPa)
1	0.28	1.38	280	0.24	1.01	2.0
2	0.24	1.37	50	0.22	1.01	2.2
3	0.22	1.38	55	0.23	0.60	2.0
4	0.14	1.40	9.6	0.36	0.28	2.4
5	0.12	1.27	8.0	–	0.22	–
6	0.11	1.32	5.0	0.23	0.21	2.3
7	0.12	1.33	2.6	0.24	0.21	2.1
8	0.11	1.33	4.3	0.25	0.21	2.2
9	0.09	1.26	4.5	0.30	0.20	2.4
Approx. errors	9%	2%	25%	30%	25%	30%

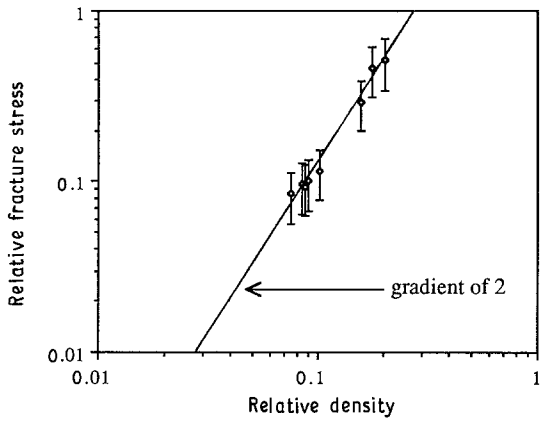

Figure 5 The log relative fracture stress as a function of log relative density. The theoretical prediction is denoted by the solid line.

proportional to the square, both terms are highly sensitive to this parameter.

Figs 4 and 5 are graphs of log relative modulus and relative fracture stress against log relative density. A least squares fit produces a gradient of 4.3 ± 1.3 (R^2 = 0.94) for the former and a gradient of 2.0 ± 0.5 (R^2 = 0.98) for the latter. This second result is in excellent agreement with the value of 2 predicted by Gibson and Ashby for closed-cell foams. In previous papers it has been stated that closed-cell foams behave as open-cell ones due to the draining of material under surface tension, which causes the cell faces to be much thinner than the cell edges. However, this is not the case for our sample foams as is clear from the two examples in Fig. 6, micrographs of three faces meeting at an edge. Thus we expect true closed-cell behaviour. Earlier experiments upon extruded maize foams [18, 19] produced results more suggestive of open-celled behaviour (i.e. a gradient of 1.5), but the results had a regression coefficient, R^2, of only 0.6 and no account of cell wall properties was taken into consideration. If we plot the log foam fracture stress against log foam density, as in the previous papers, the gradient is reduced but the error increases and the results become 1.7 ± 0.8 (R^2 = 0.96).

The gradient for the log relative modulus graph is higher than the predicted value. Nevertheless, previous results have also shown considerable scatter and it is not impossible that a power law of three is being obeyed. The size of the errors is due to the nature of Equation 4. To calculate E^* requires the difference of two nearly equal quantities in the denominator, and so the errors in this are inherently large. The original theory predicted a power of three from considering the bending stiffness of the cell faces. More recent attempts [4] to model the deformation of closed-cell foams take into account the stresses within the cell faces and the distribution of material between the faces and the edges. This leads to the following equation for the relative modulus

$$\frac{E^*}{E_s} \approx \phi^2 \left(\frac{\rho^*}{\rho_s}\right)^2 + (1 - \phi)\left(\frac{\rho^*}{\rho_s}\right) \qquad (7)$$

where ϕ is the fraction of solid contained within the cell edges. The term due to the bending of faces is no longer thought to be dominant and on the contrary is sufficiently small so as to be negligible. It can thus be seen that the simple power law for the modulus is altered and the predicted gradient is much less steep. Most, but not all, of the data collated by Gibson and Ashby support this picture. However, the data presented here definitely result in a gradient more closely in line with the original predictions, and a value which if anything is larger than three. At present there is no obvious explanation for this finding.

It would have been more satisfactory to have experimented upon a wider range of foam densities, but we were restricted by limits to the cell sizes. The lower limit was set by the fact that a piece of wall had to be extracted and have a three-point bend test performed upon it. The upper limit was set by the tendency of very thin walls to yield plastically rather than fracture, and these occurred in the large celled foams. These facts in turn limited the density range available, because high density foams tended to have small cells while the lower density foams had much larger cells, and hence both extremes were excluded from the experiments.

4. Conclusions

We have shown that the cell-wall properties of extruded starch foams vary with the extrusion conditions; in particular, the density, crystallinity and T_g. However, it was not possible to detect a significant difference between the mechanical properties of cell walls from different bulk density foams. Results show excellent agreement with the theoretical predictions

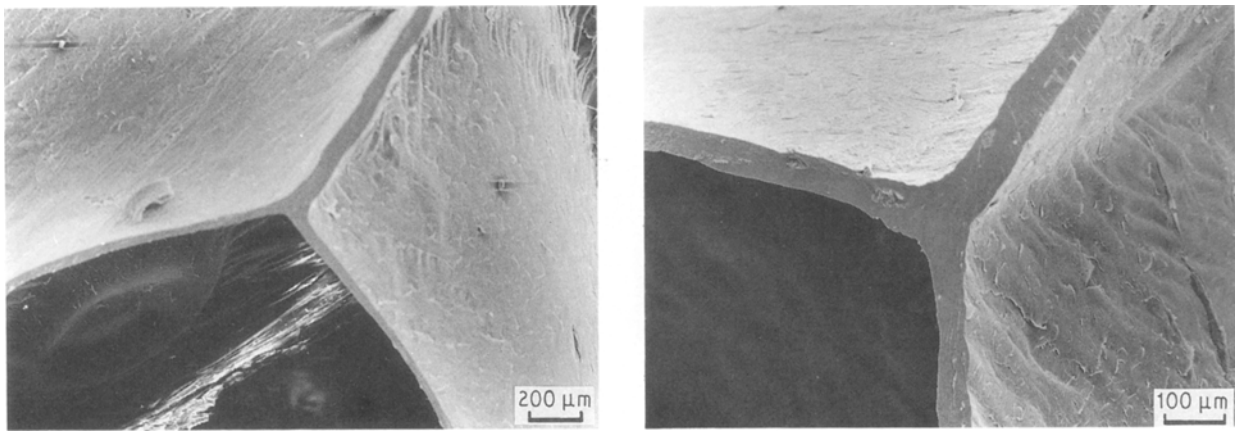

Figure 6 Scanning electron micrographs from two specimen foams showing three faces meeting at an edge.

for the variation of relative fracture stress with relative density for closed cell foams. The results for the relative modulus indicate a higher value power law than predicted.

Acknowledgements

We thank Mrs J. Ferdinand for help with making the foams and Professor M. F. Ashby for fruitful discussions. We are grateful to the S.E.R.C. and the A.F.R.C for financial support.

References

1. L. J. GIBSON, M. F. ASHBY, G. S. SCHAJER and C. I. ROBERTSON, *Proc. Roy. Soc. Lond. A* **382** (1982) 25.
2. L. J. GIBSON and M. F. ASHBY, *ibid.* **382** (1982) 43.
3. M. F. ASHBY, *Met. Trans. A* **14** (1983) 1755.
4. L. J. GIBSON and M. F. ASHBY, "Cellular Solids: Structures and Properties" (Pergamon Press, Oxford, 1988).
5. R. L. WHISTLER, J. N. BEMILLER and E. F. PASCHALL, "Starch: Chemistry and Technology" (Academic Press, Florida, 1984).
6. J. BORCH, A. SARKO and R. H. MARCHESSAULT, *J. Colloid. Interface Sci.* **41** (1972) 574.
7. R. J. PRIESTLY, *Staerke* **27** (1975) 244.
8. K. J. ZELEZNAK and R. C. HOSENEY, *Cereal Chem.* **64** (2) (1987) 121.
9. J. M. HARPER, "Extrusion of Foods" (CRC Press, Florida, 1981).
10. R. CHARBONNIERE, F. DUPRAT and A. GUILBOT, *Cereal Sci. Today* **18** (1973) 286.
11. C. MERCIER, R. CHARBONNIERE, D. GALLANT and A. GUILBOT, in "Polysaccharides in Food", edited by J. M. Blaushard and J. R. Mitchell (Butterworths, London, 1979) p. 153.
12. V. J. DAVIDSON, D. PATON, L. L. DIOSADY and G. LAROCQUE, *J. Food Sci.* **49** (1984) 453.
13. B.S. 2782, Part 3: Method 335A (1978).
14. T. J. MAURICE, L. SLADE, R. R. SIRETT and C. M. PAGE, "Influence of Water on Food Quality and Stability" (Dordrecht, Netherlands, 1985).
15. E. JONES PARRY and D. TABOR, *J. Mater. Sci.* **8** (1973) 1510.
16. P. COLONNA, J. L. DOUBLIER, J. P. MELCION, F. DE MONREDON and C. MERCIER, *Cereal Chem.* **61** (1984) 538.
17. S. H. COHEN and C. A. VOYLE, *Food Microstructure* **6** (1987) 209.
18. R. J. HUTCHINSON, G. D. E. SIODLAK and A. C. SMITH, *J. Mater. Sci.* **22** (1987) 3956.
19. A. L. HAYTER and A. C. SMITH, *ibid.* **23** (1988) 736.

Received 14 April
and accepted 29 September 1989